10th US National Combustion Meeting
Organized by the Eastern States Section of the Combustion Institute
April 23-26, 2017
College Park, Maryland

Spontaneous Ignition of Hydrothermal Flames in Supercritical Ethanol/Water Solutions

Michael C. Hicks[1,*], *Uday G. Hegde*[2], *Jun J. Kojima*[3]

[1]*NASA - Glenn Research Center, Cleveland, Ohio 44135, USA*
[2]*Case Western Reserve University, Cleveland, Ohio 44135, USA*
[3]*Ohio Aeropsace Institute, Cleveland, Ohio 44135, USA*
Corresponding Author e-mail: michael.c.hicks@nasa.gov

Abstract: Results are reported from recent tests where hydrothermal flames spontaneously ignited in a Supercritical Water Oxidation (SCWO) Test Cell. Hydrothermal flames are generally categorized as flames that occur when appropriate concentrations of fuel and oxidizer are present in supercritical water (SCW); i.e., water at conditions above its critical point (218 atm and 374 °C). A co-flow injector was used to inject fuel, comprising an aqueous solution of 30%-vol to 50%-vol ethanol, and air into a reactor held at constant pressure and filled with supercritical water at approximately 240 atm and 425 °C. Hydrothermal flames auto-ignited and quickly stabilized as either laminar or turbulent diffusion flames, depending on the injection velocities and test cell conditions. Two orthogonal views, one of which provided a backlit shadowgraphic image, provided visual observations. Optical emission measurements of the steady state flame were made over a spectral range spanning the ultraviolet (UV) to the near infrared (NIR) using a high-resolution, high-dynamic-range spectrometer. Depending on the fuel/air flow ratios varying degrees of sooting were observed and are qualitatively compared using light absorption comparisons from backlit images.

Keywords: *hydrothermal flame, supercritical water oxidation, jet injection, high pressure*

1. Introduction

The possibility of hydrothermal flames was first posited by E.U. Franck in 1985 when noting that because of the high miscibility of hydrocarbons and oxygen in supercritical water (i.e., above 218 atm and 374 °C) that "... even the generation of flames in such phases can be considered." [1] As such, a "hydrothermal flame" is a classification of flames that occur in conditions when the environment is largely comprised of water at supercritical conditions.

Historically, supercritical water oxidation (SCWO) technologies have depended on maintaining conditions in the SCWO reactor where spontaneous ignition of localized hydrothermal flames was suppressed and the complete oxidation of hydrocarbon wastes occurs at relatively low temperatures. It was recognized that these flames, if not properly controlled in reactors for which these conditions were not designed, would lead to accelerated thermal wear on reactor components, would accelerate corrosion, and depending on the reactant stream, would potentially result in increases in NOx or other unwanted products.

Recently, a number of SCWO technologies and advanced reactor concepts have been proposed where controlled hydrothermal flames are used beneficially. This includes hydrothermal flames for thermal augmentation to initiate or sustain reactions [2–4] , or as a means of increasing conversion efficiencies for traditionally difficult waste streams [5] , or for new applications, such as for hydrothermal spallation drilling [6, 7].

The purpose of this work is to explore conditions when a mixture of a proxy waste stream, (i.e. in this work, ethanol and water) is spontaneously ignited using a co-flow injection configuration where the fuel/water mixture comprise the core and air comprises the annular region of a co-flow jet. This co-flow jet is injected into supercritical water at temperatures of 425 °C and a constant pressure of approximately 240 atm. Characteristics of both laminar and turbulent hydrothermal flames, their sooting propensity as a function of flow conditions, and their measured emission spectra are studied.

2. Experimental Setup

2.1. Hardware Description

The SCWO Test Cell (Figure 1) is machined from Inconel 625 with a maximum design pressure of 340 atm at 538 °C and is typically operated at conditions up to 250 atm at temperatures up to 450 °C. The total liquid test cell volume is 57 cm^3 and consists primarily of the two orthogonal window bores 3.75 cm in diameter and 5.3 cm long. The end of each window bore is closed with a 4.13 cm diameter 2.54 cm thick sapphire window with the C-axis perpendicular to the window face.

The SCWO Test Cell (hereinafter "reactor") is heated by four electric cartridge heaters rated at 100 Watts each and located in four holes symmetrically placed around the center and in the body of the reactor. There is also an electric heater located on each of the two inlet lines to pre-heat the test fluid to temperatures just above the bulk fluid temperature before entering the reactor. The injector, as shown in the inset of Figure 1 (a) shows the arrangement of the co-flow cross-sectional areas, having a ratio of 16:1 between the annular and core flow areas.

Two cameras are used for imaging the flame and the injection hydrodynamics and the window port opposite the color camera is blanked off with a 2.54 cm thick SS-304 disc through which four thermowells, each clocked at 90 ° and protruding to varying terminal distances, are inserted. The four thermowells each accommodate a thermistor (Omega 0.59 mm RTD probes) and are used for determining the local fluid temperature. However, because of the thin flame zone, the extremely steep temperature gradients, and the thermal inertia of the thermowells the thermistors are not suitable for providing flame temperatures. In fact the difficulty of directly measuring temperatures of hydrothermal flames was noted in earlier work [8] and this will be the focus of subsequent work.

Optical emission spectroscopy was performed to measure spectral intensity in ultraviolet to near-infrared along the burner nozzle center axis at varying heights. Optical emissions were collected using a Nikon UV-Nikkor lens (105-mm, f/4.5) onto a single-core optical fiber (Ocean Optics, 0.6 mm core diameter). The light was guided into an aberration-reduced imaging spectrometer (i.e., IsoPlane 160 Princeton Instruments with a focal length 203 mm,

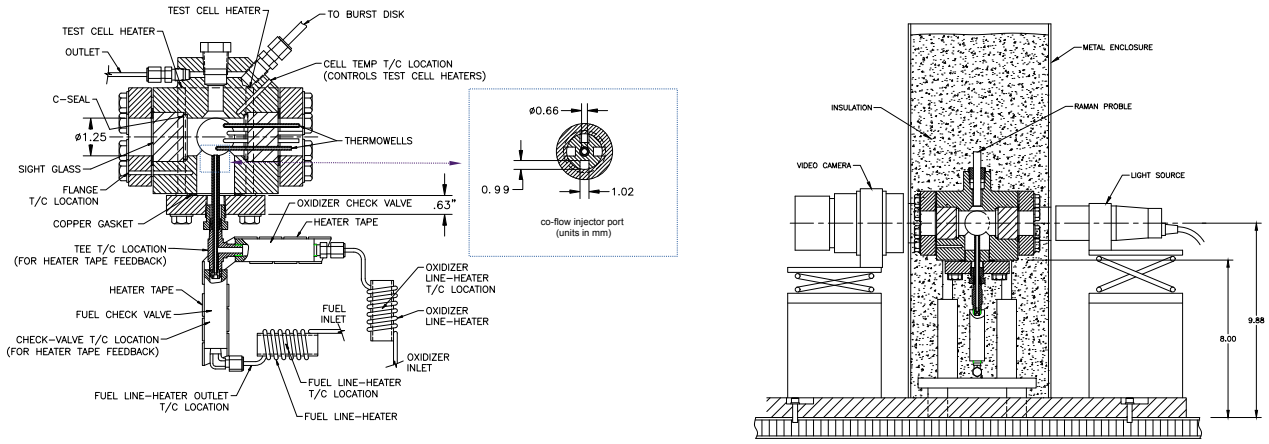

(a) (b)

Figure 1: Schematic showing (a) SCWO Test Cell in a "three window" test configuration comprising orthogonal view ports with one axis (into paper) used for back-lit shadowgraphy (collimated backlight projecting a shadow image into a high resolution B/W camera) and the orthogonal axis used for flame imaging (left side of cell) and the opposing side used for four thermowells protruding into the flame zone (b) a layout of the operational configuration showing the SCWO Test Cell packed in ceramic insulation (rotated 90° from Fig. 1(a)).

stop set at f/3.88, slit width 20 µm and grating of 300 grooves/mm) and was dispersed onto a back-illuminated imaging CCD camera (i.e., PIXIS 400BR Princeton Instruments, with a 1340×400 pixel detector and a bit depth of 16 bit). Spectral signals were binned over a height of 14 pixels and typically accumulated on CCD chip over 45 seconds to increase signal-to-noise ratio and all measurements were line-of-sight.

2.2. Experiment Procedures

For the tests reported in this work the fuel, comprising aqueous solutions of ethanol from 30%-v to 50%-v, was injected through the core and air was injected through the annulus. The reactor's bulk fluid, water, was heated to 400 °C and pressurized to 238 atm at whch point the core flow, 30%-v C_2H_6O (aq) , was initiated at 1.0 ml/min. Once the core fuel flow was stabilized the annular air flow was initiated at an initial flow rate between 1.0 ml/min to 3.0 ml/min. Following ignition the core and annular flow rates were adjusted to the targeted steady state test conditions; with flow rates independently set between 0.1 ml/min to 2.0 ml/min for each flow stream. It should be noted that the air flow was adjusted manually with a precision metering valve and was difficult to precisely determine at low flow rates due to the limitations of the flow meter.

3. Results and Discussion

3.1. Flame Characterization

Two representative hydrothermal flames are presented in Figure 2 along with the backlit images of the co-flow jets that produced them. These flames are referred to, hereinafter, simply as Flame A (Figure 2 (a) - right) and Flame B (Figure 2 (b) - right) for convenience. Both flames have a core fuel jet comprising 30%-v C_2H_6O (aq) with an annular air co-flow.

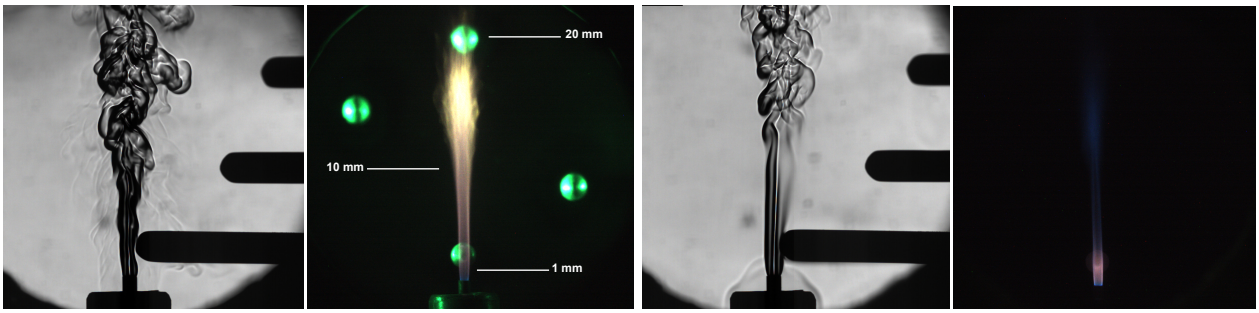

(a) (b)

Figure 2: Representative co-flow hydrothermal flames with 30%-v C_2H_6O (aq) injected from the core with air flow in the annulus; showing (a) a high flow rate air/fuel injection resulting in a partially turbulent jet and a steady state "brush" flame and (b) a reduced flow flow rate air/fuel injection resulting in a laminar jet and a weak blue flame (may be difficult to see in print).

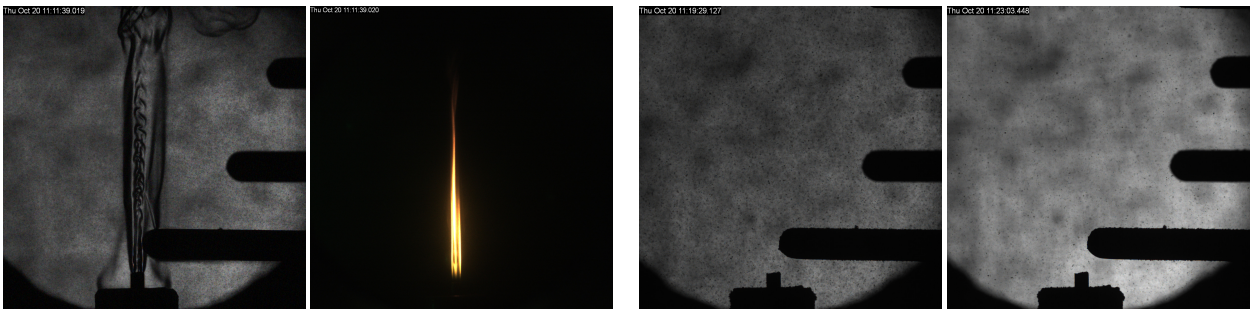

(a) (b)

Figure 3: (a) Backlit image of co-flow jet with a heavily sooting flame generated from 50%-v C_2H_6O (aq) flowing at 1.0 ml/min (core) with air flowing at 1.1 ml/min (annulus) and (b) two backlit images comparing obscuration of the collimated backlight due to the soot field immediately following flame extinction (left) and 217 s following flame extinction (right).

However, for Flame A, the air flow rate is an order of magnitude higher than for Flame B, which is evident when comparing the corresponding backlit images of the jet flow in Figure 2.

Under certain conditions hydrothermal flames can be be highly sooting, as illustrated by the flame presented in Figure 3. This shows a steady state co-flow flame with fuel, 50%-v C_2HO (aq), injected from the core at 1 ml/min with an annular air flow rate of 1.1 ml/min. The bulk fluid in the reactor was at 430 °C with a pressure of 230 atm. Soot particles were uniformly dispersed with little apparent agglomeration or settling. Following flame extinction the reactor was held at supercritical conditions for an extended period of time to observe dissolution, which appeared to occur based on qualitative comparisons of the collimated light's intensity field with time, as seen in Figure 3 (b).

3.2. Flame Spectra

Spectral measurements of flame emissions, although generally not quantitative, can provide useful insights into reactant mixing, reaction speciation, and reaction rates during combustion processes with a relatively simple diagnostic setup. Flame spectral emission measure-

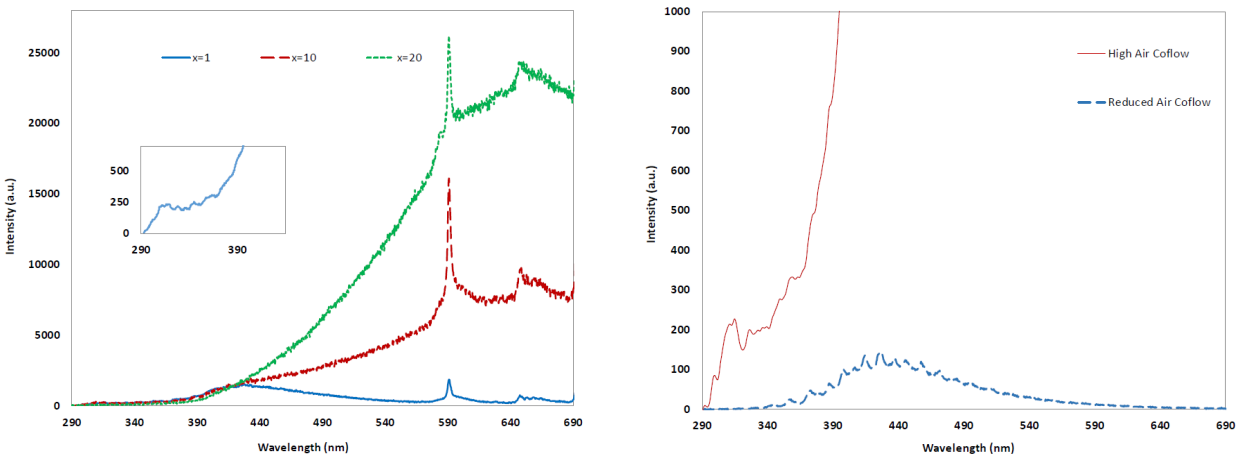

(a) (b)

Figure 4: (a) Optical emission spectra from the hydrothermal flame, measured at various axial locations from x = 1 mm to 20 mm where inset shows peak of OH* chemiluminescence at x = 10 mm and (b) optical emission spectra from the hydrothermal flame, measured at an axial location of x = 15 mm for different air coflow volumetric flow rates.

ments, briefly described in Section 2.1, are presented for Flame A and Flame B presented earlier in Figure 2 (a) and Figure 2 (b).

Emission spectra for Flame A in the wavelength range of 290 nm to 690 nm are shown in Figure 4 (a) for three heights above the burner tip, i.e., for x = 1 mm, 10 mm, and 20 mm. Consider first the spectrum at x = 1 mm which is at the base of the flame where it appears blue, Figure 2 (a). Broadband emission is observed in the wavelength range of 350 to 540 nm and is generally attributed to CO_2*, which may arise from a recombination of CO with an O atom or collisional excitation of a CO_2 molecule from its ground state. It is likely that CH* emission is masked by the CO_2* emission. The line at 590 nm is due to sodium and is likely the result of contamination of the air stream. A weak OH* signal (around 310 nm) is observed as shown in the inset. At the locations x = 10 mm and x = 20 mm the spectrum is dominated by broadband emissions above 400 nm which is likely due to black body radiation from soot. This emission is much stronger at x = 20 mm which is in the yellow turbulent brush of the flame.

Flame B is a blue non-sooty flame (may be difficult to see in print) and its emission spectra is shown for a single height (x = 10 mm) in Figure 4 (b). This location is in the blue turbulent brush region of the flame and the CO_2* emission bands are observed in the 350 nm to 540 nm wavelength range. There is no sodium line at 590 nm, which is consistent with the likelihood of it being a contaminant in the air line since the air flow rate is significantly lower for Flame B compared to Flame A. The emission spectra for Flame A, taken at the same height of 15 mm above the burner tip is also shown. Comparison of the two spectra highlight the observation that no OH* emissions or significant broadband emissions from soot are observed for Flame B. The general conclusion is that Flame B is much weaker in intensity compared to Flame A and, considering the apparent lack of OH* or soot, there may be significant differences in reaction pathways.

4. Conclusion

Results are reported from recent tests where hydrothermal flames spontaneously ignited in a Supercritical Water Oxidation (SCWO) Test Cell. A co-flow injector was used to inject fuel, comprising an aqueous solution of 30%-vol to 50%-vol ethanol and air into a reactor held at constant pressure and filled with supercritical water at approximately 240 atm and 450 °C. Optical emission measurements of the steady state flames were made over a spectral range spanning the ultraviolet (UV) to the near infrared (NIR). Depending on the fuel/air flow ratios varying degrees of sooting were observed. Future work will provide additional flame emission measurements to identify dominant reactant species, flame temperature measurements, and data on soot morphology and size distributions of these hydrothermal flames.

Acknowledgements

This work is funded under the Physical and Life Sciences Program managed by Francis P. Chiaramonte at NASA Headquarters and managed locally by William M. Foster at NASA - Glenn Research Center. The authors would like to acknowledge the significant contributions of Daniel J. Gotti for his engineering support during the hardware design and assembly phase as well as his continued support during the conduct of these tests. The authors would also like to acknowledge the contributions of Jay C. Owens for his engineering design of the imaging and data storage system.

References

[1] E. U. Franck. Aqueous mixtures to supercritical temperatures and at high pressures. *Pure and Applied Chemistry*, 57(8):1065–1070, 1985.

[2] B. Wellig, K. Lieball, and Ph. Rudolf von Rohr. Operating characteristics of a transpiring-wall {SCWO} reactor with a hydrothermal flame as internal heat source. *The Journal of Supercritical Fluids*, 34(1):35 – 50, 2005.

[3] P. Cabeza, J.P.S Queiroz, S. Arca, C. Jiménez, A. Gutiérrez, M.D. Bermejo, and M.J. Cocero. Sludge destruction by means of a hydrothermal flame. optimization of ammonia destruction conditions. *Chemical Engineering Journal*, 232:1 – 9, 2013.

[4] J.P.S. Queiroz, M.D. Bermejo, F. Mato, and M.J. Cocero. Supercritical water oxidation with hydrothermal flame as internal heat source: Efficient and clean energy production from waste. *The Journal of Supercritical Fluids*, 96:103 – 113, 2015. Workshop on Supercritical Fluids and Energy - Campinas, Brazil 2013and 25th Year Anniversary of the Journal of Supercritical Fluids.

[5] Pablo Cabeza, M. Dolores Bermejo, Cristina Jiménez, and M. José Cocero. Experimental study of the supercritical water oxidation of recalcitrant compounds under hydrothermal flames using tubular reactors. *Water Research*, 45(8):2485 – 2495, 2011.

[6] M. J. Schuler, T. Rothenfluh, P. Stathopoulos, D. Brkic, and Ph. Rudolf von Rohr. Supercritical water jets penetrating subcritical water - application for hydrothermal spallation drilling. 2012.

[7] T. Meier, D. Brkic, M. J. Schuler, M. Kant, and Ph. Rudolf von Rohr. The potential of hydrothermal flames to induce spallation in gneiss. *Proceedings World Geothermal Congress 2015*, 2015.

[8] W. Schilling and E. U. Franck. Combustion and diffusion flames at high pressures to 2000 bar. *Berichte der Bunsengesellschaft für physikalische Chemie*, 92(5):631–636, 1988.